

Improving Homogeneity for MRI RF Field at 3T Using a Huygens' Box

Chen Xue, Gabriel G. L. Zhou and Alex M. H. Wong
 State Key Laboratory of Terahertz and Millimeter Waves

Dept. of Electrical Engineering, City University of Hong Kong, Hong Kong SAR, China
 *alex.mh.wong@cityu.edu.hk

Abstract—RF magnetic (B1⁺) field homogeneity is essential to obtain high-quality magnetic resonance (MR) images. Whereas the recent advent of high field MRI makes it very difficult to achieve B1⁺ field homogeneity with traditional RF coils, we hereby propose an active metasurface-enabled scheme to achieve B1⁺ field homogeneity for 3T MRI. After explaining our methodology, we present simulation results which show superior B1⁺ field uniformity in both longitudinal and transverse cross-sections, compared to a traditional birdcage coil at the same frequency and phantom sizes.

Keywords—Metamaterial; Huygens' metasurface; MRI; ultra high field MRI; RF field homogeneity

I. INTRODUCTION

Magnetic resonance imaging (MRI) has been a common non-invasive imaging modality in the fields of anatomy, physiology, medical science and healthcare. MRI involves an RF magnetic field excitation at the Larmor frequency ω_L , which causes the precession of neutrons within the imaged subject [1]:

$$\omega_L = \gamma B_0, \quad (1)$$

where γ is the magnetic spin ratio and B_0 is the static magnetic flux density. Recent trends in MRI involve the usage of high or ultra-high static magnetic fields (3T or 7T) to improve the SNR and resolution of the MR image. The birdcage coil, which is widely used as the RF coil in MRI systems, produces a highly homogeneous B1⁺ field for low-field systems [2], but suffers B1⁺ field inhomogeneity when the frequency rises from 64 MHz (1.5T) to 127.7 MHz (3T) due to the increased electrical size of the coil [3]. In this paper, we use the Huygens' box to generate a uniform B1⁺ field in HF and UHF MRI. Through the direct application of EM equivalence, we use an active metasurface surrounding the MRI bore to excite a circularly polarized plane wave (which has perfect B-field uniformity) within the bore. A comparison of simulation results shows that our proposed MRI system achieves superior B1⁺ field uniformity at 3T compared to the field generated by the conventional birdcage coil.

II. METHDOLODY

A. Concept and Theoretical Derivation of the Huygens' box

Fig. 1 describes the concept of the Huygens' box [4][5]. As shown in Fig. 1(a), \mathbf{J}_s and \mathbf{M}_s are the electric and magnetic

surface currents placed at the boundary, and $\{\mathbf{E}_a, \mathbf{H}_a\}$ and $\{\mathbf{E}_b, \mathbf{H}_b\}$ are the EM field inside and outside the box respectively. The boundary conditions are

$$\begin{aligned} \mathbf{J}_s &= \hat{\mathbf{n}} \times (\mathbf{H}_b - \mathbf{H}_a) \\ \mathbf{M}_s &= -\hat{\mathbf{n}} \times (\mathbf{E}_b - \mathbf{E}_a) \end{aligned} \quad (2)$$

where $\hat{\mathbf{n}}$ is the normal unit vector labelled in Fig. 1 (a). In a shape enclosed by a perfect conductor (PEC), electric surface currents are shorted, and magnetic currents can be implemented by running an electric current I_a close to the conductor [4].

$$I_a = j \frac{2CAM_S}{w\mu_0\omega} \quad (3)$$

where A is the equivalent area covered by a current strip, C is a constant with the unit m^{-1} and w is the distance between the electric current I_a and the perfect conductor. Fig. 1(b) shows a model of the active Huygens' metasurface element [4].

As shown in Fig. 2, the Huygens' box we propose is the MRI bore – a cylinder with $D = 1$ m and $H = 2.3$ m. The Huygens' box features discrete current strips to synthesize the current distribution $I_a(x, y, z)$ at the boundary of the MRI bore. Current strips with $l = 50$ mm are placed in a ring formation, 45° (392 mm center-to-center) apart in the circular cross-section, with $\lambda/8$ (293.6 mm) separation between rings. Details on current strip placement choices will be given in a forthcoming paper. The current I_a at each current strip location can be found through (2) and (3), by setting $\{\mathbf{E}_b, \mathbf{H}_b\}$ to zero and $\{\mathbf{E}_a, \mathbf{H}_a\}$ as EM field distribution of the desired circularly polarized plane wave.



Fig. 1. (a) A diagram illustrating the equivalence principle. (b) A simple active Huygens' metasurface element with a perfect conductor.

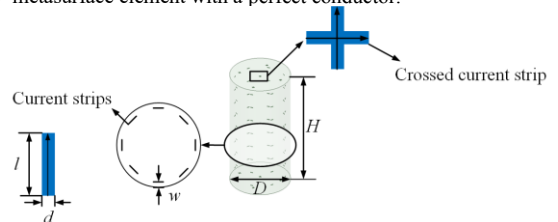


Fig. 2. The diagram of the Huygens' box.

B. Concept and Theoretical Derivation of the Birdcage coil

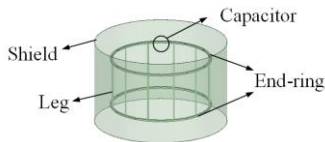


Fig. 3. The model of the high pass birdcage coil.

We compare our box to a birdcage coil shown in Fig. 3, which is reproduced from [6]. This birdcage coil has 12 legs, two end-rings and a metallic shield. Its salient parameters are given as follows: the coil diameter is 60 cm, its legs are 30 cm long and 1 cm in diameter, the external shield is 50 cm tall and 80 cm in diameter, and the tuning capacitances are 9.8 pF.

C. Simulation and Results

We show the magnetic field within cross-sections of the birdcage coil in Fig. 4 (a) and (b). As shown, the birdcage coil can generate a circularly polarized H field, but it has a varying strength across the transverse cross-section. Particularly, the field strength increases at the boundary of the coil. Additionally, Fig. 4 (c), which plots the axial cross-section of the H field, shows that the H field strength also decreases in the axial direction, away from the center of the coil. Fig. 5 shows corresponding plots of the magnetic field generated within the 3T Huygens' box. When compared to the H field in the birdcage coil, the one in the Huygens' box is more homogeneous whether it is in the transverse or the longitudinal cross-section. Both of the diameter of the transverse cross-section are 60 cm.

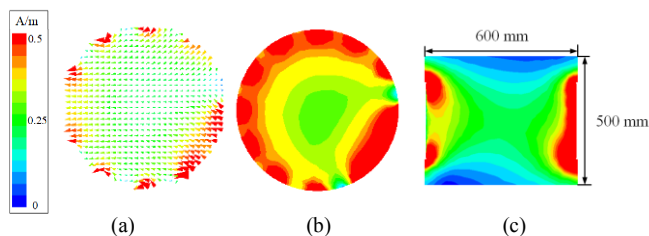


Fig. 4. (a) The vector H field and (b) The complex magnitude of H field in the transverse cross-section of the birdcage coil. (c) The complex magnitude of H field in the longitudinal cross-section of the birdcage coil. The longitudinal and the transverse cross-section both cross the center of the coil.

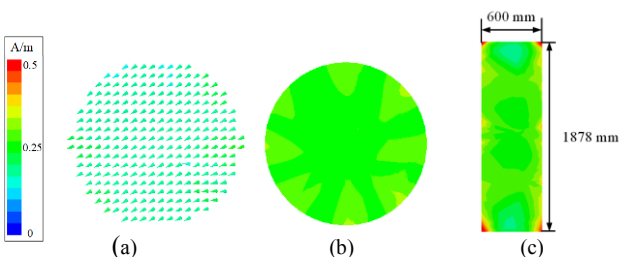


Fig. 5. (a) The vector H field and (b) The complex magnitude of H field in the transverse cross-section of the Huygens' box. (c) The complex magnitude of H field in the longitudinal cross-section of the Huygens' box. The longitudinal and the transverse cross-section both cross the center of the Huygens' box.

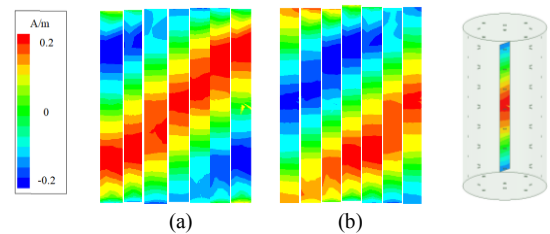


Fig. 6. (a) The x and (b) The y component of H field at $0^\circ, 30^\circ, 60^\circ, 90^\circ, 120^\circ, 150^\circ, 180^\circ$ at the longitudinal cross-section of the Huygens' Box.

Fig. 6 gives the x and y component of H field at 7 different phases at the axial cross-section of the Huygens' box. The phase difference between H_x and H_y inside the Huygens' box is about 90° and H_x is phase-lead. This verifies that the EM field is right circularly polarized. Remarkably, the EM field in the Huygens' box travels along the axial direction and does not suffer appreciable reflection at the top edge of the Huygens' box. This guarantees $B1^+$ field uniformity in the axial direction. Whereas the field within the birdcage coil changes drastically when the electrical size of the cage increases, the generation of waveform features within the Huygens' box does not depend on a certain box size, making the proposed method equally applicable to UHF MRI at 7T or even higher B_0 field strengths.

III. CONCLUSION

This paper gives a method based on the Huygens' box to solve the problem of the inhomogeneity of the $B1^+$ generated by RF coils in the MRI system. The proposed Huygens's box can generate the homogeneous $B1^+$ field both in the transverse and the longitudinal cross-section because the field inside the Huygens' box is the right circularly polarized travelling plane wave. As the Huygens' box is highly customizable, and performs better with increasing frequency, the strong applications in HF/UHF MR imaging can be expected.

REFERENCES

- [1] M. Jo, M. Lupu, and A. Briguet. NMR probeheads for biophysical and biomedical experiments: theoretical principles & practical guidelines. Imperial College Press, pp.3.2006.
- [2] C. E. Hayes, W. A. Edelstein, J. F. Schenck, O. M. Mueller, and M. Eash, "An Efficient, Highly homogeneous radiofrequency coil for whole-body Nmr imaging at 1.5-T," J. Magn. Reson., vol. 63, pp. 622-628, 1985.
- [3] P. Roschmann, "Radiofrequency penetration and absorption in the human-body - limitations to high-field whole-body nuclear-magnetic-resonance imaging," Med. Phys., vol. 14, pp. 922-931, 1987.
- [4] A. M. H. Wong, and George V. Eleftheriades. "Active Huygens' box: metasurface-enabled arbitrary electromagnetic wave generation inside a cavity." arXiv:1810.05998 (2018).
- [5] A. M. H. Wong and G. V. Eleftheriades, "Experimental demonstration of the Huygens' box: arbitrary waveform generation in a metallic cavity", 2018 IEEE International Symposium on Antennas and Propagation & USNC/URSI National Radio Science Meeting, Boston, MA, 2018, pp. 1893-1894.
- [6] Pisa, et al., "Interaction between MRI RF field and pacemaker holders: A comparison between birdcage and TEM coils in 3 T systems," Proceedings of the 5th European Conference on Antennas and Propagation, Rome, 2011, pp. 1942-1945.